J Mater Sci: Mater Med (2006) 17:691–695
DOI 10.1007/s10856-006-9679-7

Preparation of fluoride-substituted hydroxyapatite by a molten salt synthesis route

Hui Gang Zhang · Qingshan Zhu

Received: 21 March 2005 / Accepted: 21 October 2005

Abstract Fluoride-substituted hydroxyapatite (FHAp) with high thermal and morphologic stability was successfully prepared by a molten salt synthesis route. XRD patterns and FTIR spectra identified the synthesized powders as FHAp solid solution. The FHAp obtained with potassium sulfate as the flux showed the rod-like morphology without detectable decomposition up to 1300°C and the flux, sodium sulfate, led to the spheriodal FHAp. After investigating the effects of salt species on the FHAp morphologies, it was found that solubility was not the exclusive factor, which affected the morphological development of apatite powders, and the cations of molten salt species also played an important role.

1. Introduction

Fluoride-substituted hydroxyapatite (FHAp) has been increasingly investigated as clinical restoration materials for stimulatory purposes in hard tissues or for maintaining the stability of materials during processing. It was reported that FHAp could provide sufficiently low levels of fluoride to act upon the surrounding cells for improving bone formation, while avoiding unnecessary accumulation within the body [1–2]. Various types of FHAp ceramics including powdery and sintered forms as well as coating on metals were developed in the past century. Since the morphologies of inorganic powders have much influence upon their properties and applications [3–4] and both thermal and morphological stability affects the long-term performance problem of hydroxyapatite coatings on ceramic or metallic implants due to decomposition during processing [5], to prepare morphologically varied FHAp powders with high stability is of value and interest. Wet methods, which are most commonly used, result in relatively inferior crystallinity, thermal [6–8] and morphological stability [9–10]. Hydrothermal and solid-state reactions, which involve comparatively high temperatures, are proven relatively complicated and difficult to control morphology [6]. Thus, to synthesize the morphologically varied FHAp with high stability, a new and simple route is needed.

Molten salt synthesis (MSS) does not require precise control over synthesis conditions [10–11], and has been successfully applied to synthesize many ceramic powders [10–15] with various morphologies. Thus, the purpose of this work is to explore the preparation of FHAp powders with the thermal and morphological stability via a molten salt synthesis route and to investigate the factors, which affect the morphologies of FHAp powders. We successfully synthesized rod-like FHAp with K_2SO_4 as the flux and spherical FHAp with Na_2SO_4.

2. Experimental

The starting materials including hydroxyapatite (HAp), tricalcium phosphate (TCP), and calcium fluoride (CaF_2), potassium sulfate (K_2SO_4, melting point, 1069°C), potassium chloride (KCl, melting point, 771°C), and sodium sulfate (Na_2SO_4, melting point, 884°C), were purchased from Beijing Chemicals Corp., China. Fluoride-substituted hydroxyapatite, $Ca_5(PO_4)_3(OH)_{1-x}F_x$, with $x = 0, 0.25, 0.50,$

H. G. Zhang
Multiphase Reaction Laboratory, Institute of Process Engineering, Chinese Academy of Sciences, P.O. Box 353, Beijing 100080, P.R. China; Graduate School of the Chinese Academy of Sciences, Beijing 100039, P.R. China

Q. Zhu (✉)
Multiphase Reaction Laboratory, Institute of Process Engineering, Chinese Academy of Sciences, P.O. Box 353, Beijing 100080, P.R. China;
e-mail: qszhu@home.ipe.ac.cn

0.75, 1.0, were respectively synthesized and referred to as FHA00, FHA25, FHA50, FHA75, and FHA100, hereafter. According to the reaction formula, $(1–x)\ Ca_5(PO_4)_3(OH) + 1.5x\ Ca_3(PO_4)_2 + 0.5x\ CaF_2 \rightarrow Ca_5(PO_4)_3(OH)_{1-x}\ F_x$, the amount of each reactant with total weight of 8 g was calculated for different degree of fluoridation. The reagents with the predetermined composition and the flux were weighted and placed in alumina crucibles. The mixture obtained was heated to 880∼1190°C and held for 4 hours in a box furnace. After the furnace was cooled naturally to room temperature, the solidified samples were immersed into deionized water, which was vigorously stirred at 80°C until the samples broke into fine powders. After washing several times with hot deionized water (∼80°C) until the specific conductance of the decanted liquid fell to $< 2.4\mu$S, the fine powders were filtered by using a Buckner funnel and dried at 80°C for 24 hours. The solubility of FHAp in different flux was determined according to the previously reported method [13]. The FHAp pellets sintered at 1100°C were embedded in a flux at desired temperatures for 2 hours. The solubility was calculated by the weight differences of the FHAp pellets before and after heating.

The phase constitutions of the as-synthesized powders were identified by an X-ray diffractometer (XRD, D/MAX 2500X, Rigaku, Japan) with Cu$K\alpha$ radiation. The morphologies were examined by scanning electron microscopy (SEM, JSM-35 CF, JEOL, Japan) and field emission scanning electron microscopy (FESEM, JSM-6700F, JEOL, Japan). The element analyses and accurate Ca/P ratio were determined respectively by energy dispersive X-ray spectroscopy (EDS, League 2000, KYKY, China) and inductively coupled plasma-atomic emission spectroscopy (ICP-AES, Analyst 200, Perkin-Elmer, USA). The fluoride content was measured by a fluoride ion selective electrode (PF-1, Shanghai Leici, China). Fourier transform infrared (FTIR) spectra were recorded using the KBr pellet technique in a FTIR spectrophotometer (Equinox 55, Bruker, Germany) at room temperature.

3. Results and discussion

Figure 1 shows the X-ray diffraction patterns of FHA00, FHA50, and FHA100 powders synthesized with K_2SO_4 as the flux. The patterns of FHA00 and FHA100 are

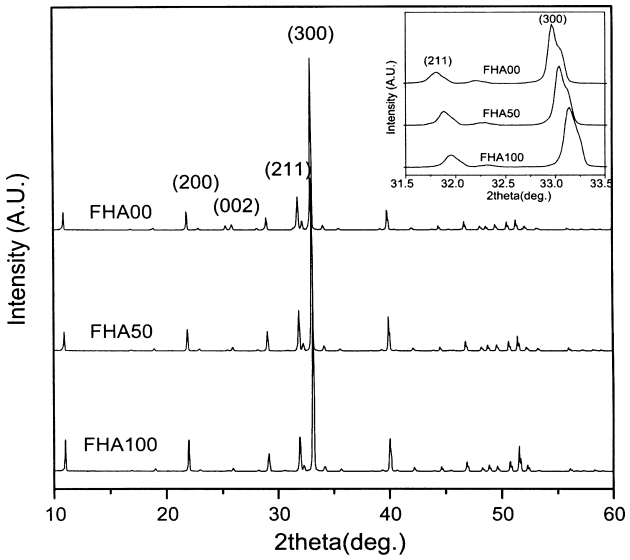

Fig. 1 XRD patterns of FHA00, FHA50, and FHA100 powders synthesized with K_2SO_4 as the flux. Experimental conditions: the mixtures with the weight ratio of K_2SO_4 to the desired FHAp, 1.6, were heated to 1190°C at the rate 5°C/min, held for 4 hours.

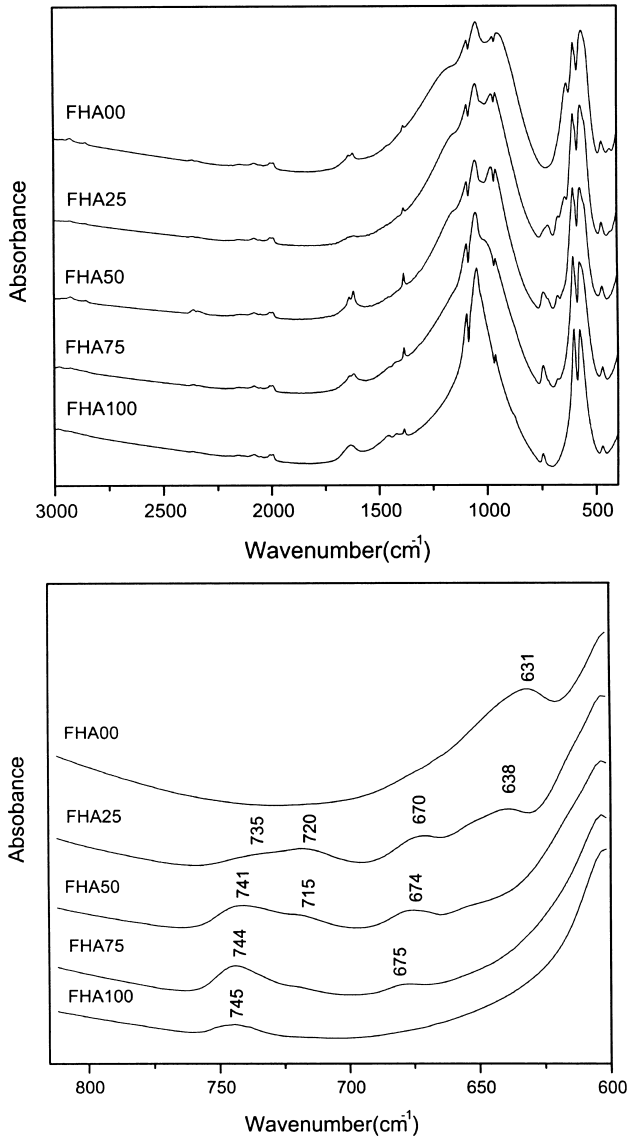

Fig. 2 FTIR spectra of the FHAp powders synthesized with K_2SO_4 as the flux. Experimental conditions: the mixtures with the weight ratio of K_2SO_4 to the desired FHAp, 1.6, were heated to 1190°C at the rate 5°C/min, held for 4 hours.

respectively consistent with those of pure hydroxyapatite (HAp, JCPDS card #9-432) and pure fluorapatite (FAp, JCPDS card #15-876). Due to whisker orientation, the intensity of the (300) planes becomes very strong and overtakes that of the (211) planes, and the peak of (002) planes become very weak, so the elongated direction may be [001]. The enlargement of 31.5∼33.5° section shows that the (300) peak shifts to right, indicating the shrinkage of a-axis length of FHAp with the increasing fluoride content. No peaks of TCP and CaF_2 were detected in XRD patterns, indicating the depletion of the starting materials.

Figure 2 shows the FTIR spectra of the as-synthesized composites. The typical phosphate vibration modes of apatite [16] appear in all samples, including the antisymmetric P-O stretching mode at the bands of 1092 cm^{-1} and 1048 cm^{-1}, the symmetric P-O stretching mode at 962 cm^{-1}, the O-P-O bending mode at the bands of 601, 564, and 472 cm^{-1}. The band at about 631 cm^{-1}, which arises from the bending motion of the OH^- chain, shifts to higher wavenumber when x increases from 0 to 0.25. Its intensity decreases gradually and disappears at $x = 0.5$. A series of peaks between 745 and 631 cm^{-1} had been assigned to diverse configurations of OH^- and F^- in the X-channel of FHAp crystals [17–19], so in conjunction with the XRD analyses, the synthesized samples can be identified as fluoride-substituted hydroxyapatite solid solutions instead of the mixtures of FAp and HAp. The weak absorption at 1420 and 1456 cm^{-1} indicates a slight B-type CO_3^{2-} substitution for PO_4^{3-} ions [19].

Figure 3 shows the SEM images of the as-synthesized FHAp samples via the MSS route. All the samples with K_2SO_4 as the flux show rod-like morphology. SEM investigations indicate that the ratio of F^- to OH^- has no significant effect on the morphology of FHAp. The mean diameter and length are respectively about 8μm and 50μm.

Several authors [5, 17, 20] reported the thermal stability of synthetic FHAp but the results were varied. FHAp with partial substitution synthesized via precipitation reactions remained thermally stable up to 900∼1300°C. Sol-gel derived FHAp coating did not decompose until 800°C [22]. As to the morphological stability, previous reports [21] showed that FHAp synthesized via precipitation reactions grew larger and transformed from prismatic crystals into spheroidal particles after calcinating at 1000°C for 1 hour. However, there are no investigations about the synthesis of FHAp with both thermal and morphological stability. The FHAp synthesized in this study was calcinated for 10 hours at 1300°C, rod-like morphology was kept completely and did not grow into spheroidal grains (Fig. 3d). The comparison of XRD patterns in Fig. 4 showed that no impure phase appeared after 10 h calcination except the significant increase of peak intensity due to well crystallization. The above SEM and XRD analyses indicated that fluoride-substituted hydroxyapatite prepared via the molten salt synthesis has high thermal and morphological stability up to 1300°C.

In order to investigate the influence of flux species upon the morphological development with the expectation for

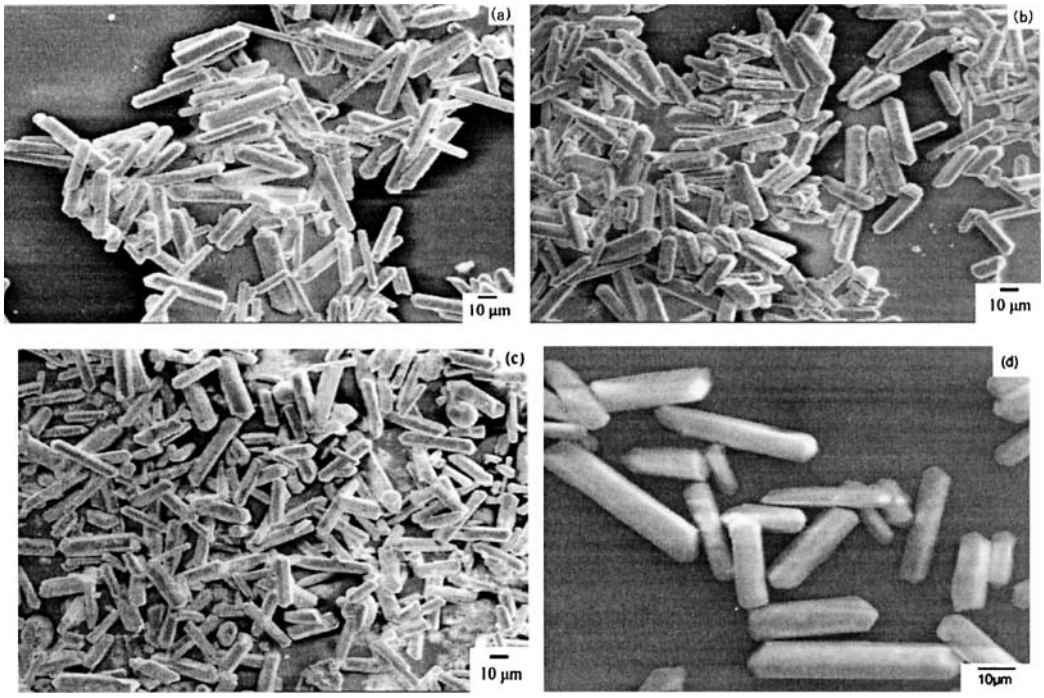

Fig. 3 SEM images of FHAp synthesized with the K_2SO_4-to-FHAp ratio of 1.6 at 1190°C: (a) FHA00, (b) FHA50, (c) FHA100, (d) FHA75 after calcinating at 1300°C.

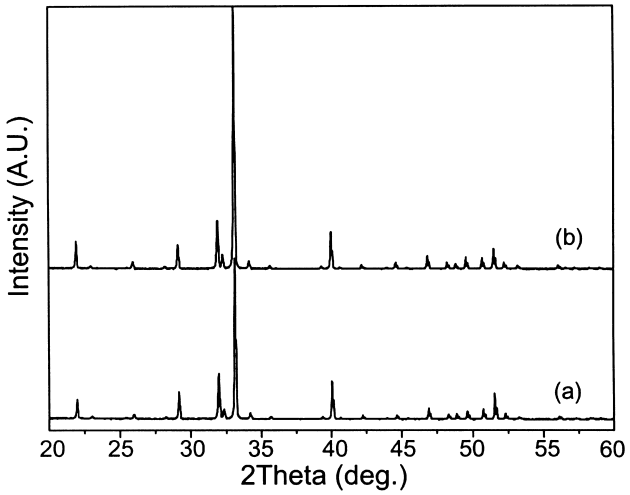

Fig. 4 XRD patterns of (a) the as-prepared FHA75 and (b) the calcinated FHA75 at 1300°C.

better morphology development, two low melting-point salts, KCl and Na_2SO_4, were also tried as the fluxes. As a result, FHAp formed in the fluxes of KCl and Na_2SO_4, and however did not develop large aspect ratios. The FESEM image in Fig. 5a showed that molten Na_2SO_4 led to the spheroidal FHAp particles with the size of ∼50 nm in contrast to ∼50 μm long rod-like particles in molten K_2SO_4, whose clear faces and edges can be seen in Fig. 5b. Since the morphology evolution was realized by mass transportation which was affected by solubility in molten salts [12], to explain the differences caused by the fluxes, KCl, Na_2SO_4, and K_2SO_4, the dissolved amounts of FHAp in these fluxes were determined. The results as listed in Table 1 apparently show that the solubility of FHAp in molten KCl is one order of magnitude lower than in molten K_2SO_4 under the given experimental conditions. The relatively small solubility of FHAp in the molten salt KCl limited the dissolution of FHAp and retarded the diffusion to the newly nucleated crystals. So this resulted in the failure of rod-like FHAp formation in the molten salt KCl. But the comparison of the cases for K_2SO_4 and Na_2SO_4 indicated that solubility was not the exclusive factor, which affected the growth habit of FHAp in molten salts, because the flux Na_2SO_4 could dissolve a considerable amount of FHAp in comparison with K_2SO_4, and however, did not help to form rod-like shape. It implied that there must be some other factors which decided the morphological development of FHAp particles.

The main difference of two flux species was their cations, so the EDS analyses were performed and the results (as shown in Fig. 5) gave the evidence that both sodium and potassium incorporated into the apatite. ICP-AES analyses showed that the FHAp prepared with K_2SO_4 as the flux contains 0.1 ∼ 0.23 wt% potassium and those powders synthesized with Na_2SO_4 as the flux contained up to 1 wt% sodium. It is evident that the uptake content of potassium ions is much less than that of sodium ions in molten salt syntheses. The fact that more sodium ions than potassium ions in aqueous solutions could be incorporated into apatite lattice has been substantiated by experimental results in many literatures [23–24]. The results of Christoffersen et al. even suggested that K^+ was not incorporated into HAp without corresponding anion substitution [25]. As Tomazic et al. reported [26], the order of uptake of alkali ions into apatite phase in aqueous solutions followed the sequence: $Li^+ > Na^+ > K^+$, due to the varied affinity for incorporation into apatite lattice. Some investigations [27–29] have proved that the incorporation of many cations into apatite lattice is responsible for the inhibition of growth in aqueous solutions. Although the exact mechanism was not clear in molten salt syntheses, as compared to ∼50 μm-long rod-like FHAp in K_2SO_4 flux, the

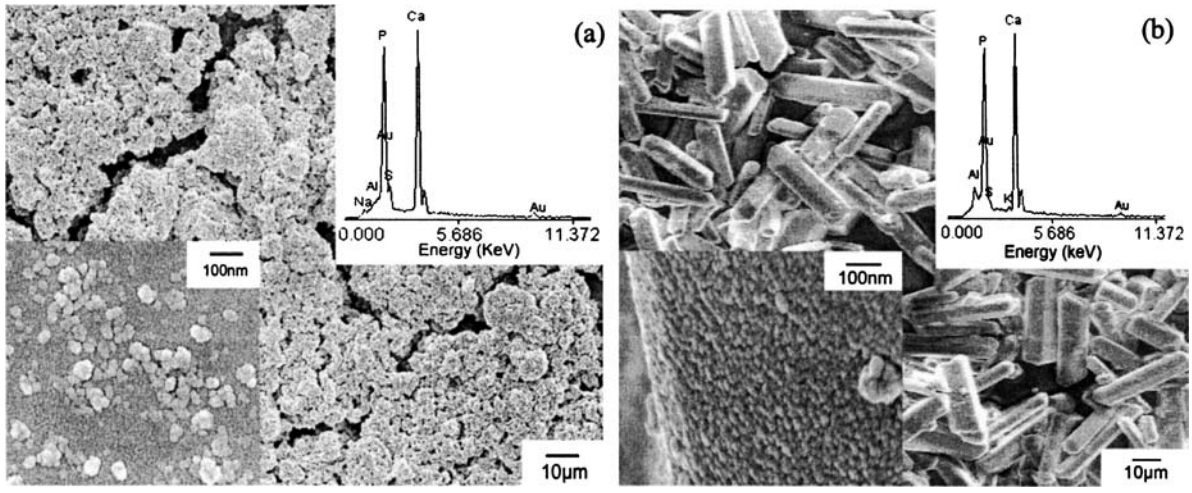

Fig. 5 SEM images and EDS spectra of the dissolved FHA75 particles (a) in molten Na_2SO_4 at 1000°C and (b) in molten K_2SO_4 at 1190°C, respectively. (The left-bottom inserts were FESEM images of the dissolved FHA75 powders from sintered pellets by Na_2SO_4 and K_2SO_4, which, after ultrasonic treatment, were dispersed on aluminum-sheet and then sputtered with gold for FESEM observation).

Table 1 Dissolved amounts of FHAp in the fluxes

Firing conditions (for 2 hours)	Dissolved amounts (mol/g of salt)
FHA75 in KCI at 880°C	3.1×10^{-6}
FHA75 in K_2SO_4 at 1190°C	5.9×10^{-5}
FHA75 in Na_2SO_4 at 1000°C	2.3×10^{-5}

growth stop of FHAp in the size of ∼50 nm with Na_2SO_4 as the flux must be related to the high incorporation of sodium. Thus, cations of molten salts must play an important role in molten salt syntheses, which differed from previous studies [10, 11].

4. Conclusion

Rod-like powders of fluoride-substituted hydroxyapatite solid solution were successfully prepared via a molten salt synthesis route. XRD patterns and FTIR spectra identified the synthesized powders as FHAp solid solution. The FHAp obtained has high thermal and morphologic stability and can keep the rod-like shapes without detectable decomposition up to 1300°C. Among the flux salts investigated, only K_2SO_4 led to rod-like FHAp, while the insufficient solubility of FHAp in molten KCl might retard the formation of rod-like shapes. The reason why Na_2SO_4 led to spheroidal morphology was attributable to the incorporation of relatively large amount of sodium ions into FHAp lattice. So solubility was not the exclusive factor which affected the morphological development and the cations of molten salts also played an important role in molten salt syntheses.

Acknowledgement We express our gratitude for the financial supports from National Natural Science Foundation of China (grant No. 20221603 and 20406023) and Chinese Academy of Sciences.

References

1. K. A. GROSS and L. M. RODRÍGUEZ-LORENZO, *Biomaterials* **25** (2004) 1385.
2. K. A. BHADANG and K. A. GROSS, *Biomaterials* **25** (2004) 4935.
3. C. BURDA, X. CHEN, R. NARAYANAN and M. A. EI-SAYED, *Chem. Rev.* **105** (2005) 1025.
4. S. MANN, *Angew. Chem. Int. Ed.* **39** (2000) 3392.
5. Y. M. CHEN and X. G. MIAO, *Biomaterials* **26** (2005) 1205.
6. C. KOTHAPALLI, M. WEI, A. VASILIEV and M. T. SHAW, *Acta Mater.* **52** (2004) 5655.
7. H. W. KIM, Y. M. KONG, C. J. BAE, Y. J. NOH and H. E. KIM, *Biomaterials* **25** (2004) 2919.
8. Z. W. YANG, Y. S. JIANG, Y. J. WANG, L. Y. MA and F. F. LI, *Mater. Lett.* **58** (2004) 3586.
9. W. SUCHANEK, M. YASHIMA, M. KAKIHANA and M. YOSHIMURA, *J. Am. Ceram. Soc.* **80** (1997) 2805.
10. A. C. TAS, *J. Am. Ceram. Soc.* **84** (2001) 295.
11. A. C. TAS, *Powder Diffr.* **16** (2001) 102.
12. K. H. YOON, Y.S. CHO and D. H. KANG, *J. Mater. Sci.* **33** (1998) 2977.
13. K. H. YOON, Y. S. CHO, D. H. LEE and D. H. KANG, *J. Am. Ceram. Soc.* **76** (1993) 1373.
14. C. C. CHIU, C. C. LI and S. B. DESU, *J. Am. Ceram. Soc.* **74** (1991) 38.
15. Y. SUETSUGU and J. TANAKA, *J. Mater. Sci.: Mater. Med.* **10** (1999) 516.
16. B. O. FOWLER, *Inorg. Chem.* **13** (1974) 194.
17. L. M. RODRLGUE-LORENZO, J. N. HART and K. A. GROSS, *Biomaterials.* **24** (2003) 3777.
18. F. FREUND and R. M. KNOBEL, *J. Chem. Soc.: Dalton Trans.* **6** (1977) 1136.
19. J. C. ELLIOTT, Structure and Chemistry of the Apatites and Other Calcium Orthophosphates. Studies in Inorganic Chemistry Vol 18, (Elsevier, Amsterdam, 1994).
20. K. KAMIYA, M. TANAHASHI, T. SUZUKI and K. TANAKA, *Mater. Res. Bull.* **25** (1990) 63.
21. M. WEI and J. H. EVANS, *J. Mater. Sci.: Mater. Med.* **14** (2003) 311.
22. H. W. KIM, Y. M. KONG, C. J. BAE, Y. J. NOH and H. E. KIM, *Biomaterials* **25** (2004) 2919.
23. E. A. P. De MAEYER, R. M. H. VERBEECK and I. Y. PIETERS, *Inorg. Chem.* **35** (1996) 857.
24. P. REGNIER, A. C. LASAGE, R. A. BERNER, O. H. HAN and K. W. ZILM, *Am. Mineral.* **79** (1994) 809.
25. J. CHRISTOFFERSEN, M. R. CHRISTOFFERSEN and N. KJAERGAARD, *J. Crystal Growth* **43** (1978) 501.
26. B. B. TOMAZIC, I. MAYER and W. E. BROWN, *J. Crystal Growth* **108** (1991) 670.
27. P. G. KOUTSOUKOS and G. H. NANCOLLAS, *Colloids Surf.* **17** (1986) 361.
28. M. KUMAR, J. XIE, K. CHITTUR and C. RILEY, *Biomaterials* **20** (1999) 1389.
29. N. KANZAKI, K. ONUMA, A. ITO, K. TERAOKA, T. TATEISHI and S. TSUTSUMI, *J. Phys. Chem. B.* **102** (1998) 6471.